DesignCon 2021

Advanced Modeling for Novel High-performing Low-cost Copper Foils

Shaohui Yong, Marvell Technology Inc.
yongsh@ieee.org

Xiaoning Ye, Intel Corporation
xiaoning.ye@intel.com

Johnny Sung, Co-tech Development Corporation
johnny.sung@co-tech.com

Frank Lee, Co-tech Development Corporation
frank_lee@co-tech.com

Jun Fan, Missouri University of Science and Technology
jfan@mst.edu

Abstract

In recent years, the Huray model based on pyramidal stacked spheres on a smooth surface, has gained popularity. However, in practice, it is very difficult to determine the parameters of the model. Furthermore, Huray model's assumption of no interaction among the stacked spheres can potentially result in large modeling error. A new modeling approach relating the cross-sectional profile of the surface roughness and the surface roughness correction factor is developed by introducing a 3D full-wave simulation of a transmission line with surface roughness. Meanwhile, simulation and measurement correlation for four types of copper foil are studied using the newly proposed method. Among the four types of copper foils, three are new types of non-conventional copper foils with high performance and lower cost than conventional copper foils such as HVLP and HVLP2.

Author(s) Biography

Shaohui Yong received the M.S. and Ph.D. degrees in electrical engineering from the Missouri University of Science and Technology, Rolla, MO, USA, in 2015 and 2020, respectively. He is currently a Staff Engineer at Marvell Technology, Santa Clara, CA, USA, responsible for signal and power integrity of high-speed integrated circuit packaging. His research interests are in the areas of electromagnetic measurement and simulation techniques, integrated circuit packaging, and high-speed digital systems.

Xiaoning Ye is currently a Principal Engineer at Intel Corporation, responsible for signal integrity of high-speed interconnects in server systems. He received his Bachelor and Master Degrees in electronics engineering from Tsinghua University, Beijing, China, in 1995 and 1997 respectively, and the Ph.D. degree in electrical engineering from University of Missouri – Rolla (currently Missouri University of Science and Technology) in 2000. Dr. Ye has published over 100 IEEE and other technical papers, and holds 15 patents and a few more patent applications. Dr. Ye is currently member of board of directors of EMC society, and served as chair of the Technical Advisory Committee for IEEE EMC Society in 2018-2020. He also chaired IEEE 370 standard development workgroup, and IPC D24D task force. Dr. Ye received Technical Achievement Award from IEEE EMC Society in 2015.

Johnny Sung received M.S. degree in Environmental Engineering from National Chung Hsing University. Currently, he is the R&D director at Co-Tech Corporation. He took the destructive innovation approach and successfully developed RG311/RG312 foil with comparable signal integrity performance to HVLP foil. He is focusing on surface microstructure engineering and signal integrity. His most recent publications can be found in APEMC 2019.

Frank Lee received B.S. Degree in business administration from National Chengchi University. He has been Co-Tech Copper Foil's president since 2014. Frank has 38 years experiences in electrochemical materials, high power systems, info networking solutions and consumer electronics products.

Jun Fan (Fellow, IEEE) received B.S. and M.S. degrees in electronic engineering from Tsinghua University, Beijing, China, in 1994 and 1997, respectively. He received the Ph.D. degree in electrical engineering from the University of Missouri-Rolla, Rolla, MO, USA, in 2000., From 2000 to 2007, he worked with NCR Corporation, San Diego, CA, USA, as a Consultant Engineer. In July 2007, he joined the Missouri University of Science and Technology (formerly the University of Missouri-Rolla) and became a Tenured Professor in 2016. He was also a Senior Investigator with the Missouri S&T Material Research Center. From 2013, he has served as the Director for the Missouri S&T EMC Laboratory and the Director for the National Science Foundation (NSF) Industry/University Cooperative Research Center (I/UCRC) for Electromagnetic Compatibility (EMC). From October 2018, he has been the Cynthia Tang Missouri Distinguished Professor in Computer Engineering. His research interests include hardware design and fundamental research for electromagnetic compatibility (including signal and power integrity) at the levels of integrated circuit, package, PCB, and system, and the development of specialized design tools and innovative measurement technologies., Dr. Fan served as a member of the Board of Directors, the Chair of the Technical Advisory Committee, the Chair of the TC-9 Computational Electromagnetics Committee, and a Distinguished Lecturer. He currently is an Associate Editor for the IEEE Transactions on Electromagnetic Compatibility and IEEE Electromagnetic Compatibility Magazine. He was the Technical Paper Chair and Technical Program Chair for a few IEEE International Symposia on Electromagnetic Compatibility, the General Chair for IEEE International Conference on Signal and Power Integrity, the Founding Chair for the SC-4 EMC for Emerging Wireless Technologies Special Committee, and so on. He received an IEEE Transactions on Electromagnetic Compatibility Society Technical Achievement Award in August 2009.

Introduction

As the data rate of digital systems is getting higher, the frequency-dependent attenuation of the interconnection becomes one of the most important factors that are bottlenecking the signal integrity performance of the high-speed design [1-3]. The conductor loss due to surface roughness has become a research topic for the past decade. The Huray model has been presented to account for this issue [4]. However, the Huray model's implementation and accuracy are still challenging for engineers since determining the model parameters has always been a problem. In recent years, to solve the parameters tuning problem for Huray model some approaches were developed [5][6], but empirical estimation or fitting is still required for the following reasons. Firstly, the diameter and number of spheres "inside" the pyramidal stacks are not measurable by scanning electron microscope (SEM). Secondly, the Huray model assumes no interaction among the stacked spheres. The spheres shielded or hidden beneath other spheres are supposed to account for less loss than the spheres fully exposed to the wavefront [7]. However, for Huray model the loss of the pyramidal stack is calculated by the superposition of power absorbed from each sphere completely exposed to the incident wave. To investigate the interaction among conductive structures, the total absorption of the stacked spheres is simulated using a method of moments (MoM) solver. Compared to the simulation results, we found that the estimation assuming negligible interaction among spheres severely overestimates the total absorption. Thus, theoretically it is questionable that an accurate Huray model can be built by extracting parameters only through observing SEM images. A new surface roughness modeling methodology with improved accuracy should be developed to account for the surface-area exclusion.

The objective of the project is to determine the electrical performance of copper foil applied to a certain fabricated printed circuit board (PCB) by relating the surface roughness correction factor to the measured conductor surface roughness profile under test. To achieve improved accuracy of the surface roughness model, in this project we are going to introduce the 3D full-wave simulation of the rough surface by observing the cross-sectional SEM image of the transmission line, instead of guessing parameters of Huray model empirically. Inspired by the essence of Huray model that the additional signal loss is approximately proportional to the increased surface area (due to the copper nodules) per unit area, the 3D rough surface to be simulated is generated by modeling both the statistical protrusion height and cross-sectional profile length information, assuming that the roughness level along and perpendicular and parallel to the signal propagation direction is uniform. At last, the 3D rough surface is implemented into the transmission line model and the surface roughness correction factor is obtained.

To test the proposed surface roughness modeling approach, testing vehicles are built using four different copper foil types (from rough copper to extremely smooth copper). The SEM foil surface image is processed by an in-house image identification software, and information about smaller spheres in a certain area is obtained. The height of the protrusions is analyzed statistically, and the cross-sectional profile of the foil surface is obtained. The 3D models with different rough surfaces are generated and simulated.

The measurement data (including S-parameters, cross-sectional profile, SEM surface image) from testing vehicles are analyzed. We use the advanced modeling approach proposed in this paper to validate the accuracy of the proposed methodology. A detailed comparison between the modeling results and measurement is presented.

We found that new types of copper foil with shorter profile length and statistical protrusion height non-uniform surface roughness have less insertion loss. Although this new type of "advanced Reverse Treatment Foil (RTF)" copper foil has some large copper nodules at a certain area as big as regular RTF, the over increased surface area is averaged out per unit area thanks to relatively flat profile in other areas. Therefore, the loss performance degradation due to the advanced RTF copper is much less than the regular RTF. However, the manufacturing cost of advanced RTF is much lower than other high-performance copper profiles such as Hyper Very Low Profile (HVLP) or HVLP2.

Foil Roughness Modeling with Uniform Spheres

Before introducing the proposed modeling approach, we would like to take a look at the derivation of the Huray model's surface roughness correction factor and introduce some necessary parameters. As Figure 1. illustrates, the rough surface is modeled by adding spheres to a smooth conductive plane.

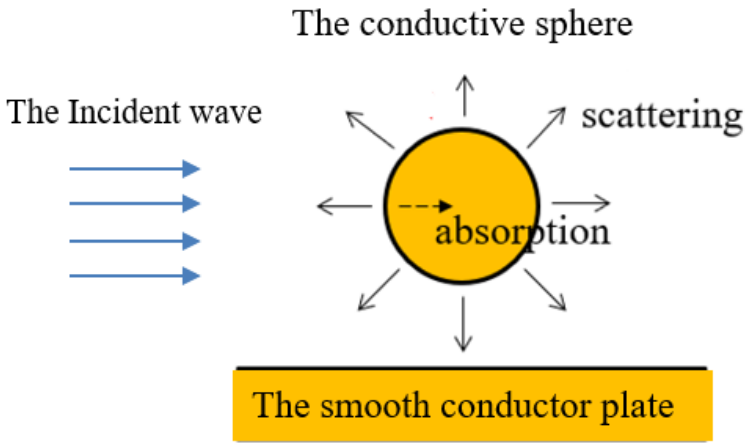

Figure 1. Scattering and absorption of a conducive sphere.

The incident plane wave's Poynting vector is expressed as [8, (26)]:

$$S = \frac{1}{2}|E_0| \cdot |H_0| = \frac{1}{2}\eta |H_0|^2$$

where $|E_0|$ and $|H_0|$ are the magnitude of the magnetic and electric field. The impedance is defined using $\eta = \sqrt{\mu_0/\varepsilon_0\varepsilon_r}$. The total cross-section of a sphere (σ_{total}) is the superposition of scattering (σ_{sca}) and absorption cross-section (σ_{abs}) [9, (10.62)]:

$$\sigma_{total} = \sigma_{sca} + \sigma_{abs}$$

As [4, Fig.18] demonstrated, within the bandwidth from 1MHz to 100GHz, scattering is almost negligible compared to absorption ($\sigma_{sca} \ll \sigma_{abs}$) for the spheres with radius smaller than 1μm. Thus, we assume that the total cross-section of the sphere is equal to its absorption cross-section ($\sigma_{total} \approx \sigma_{abs}$).

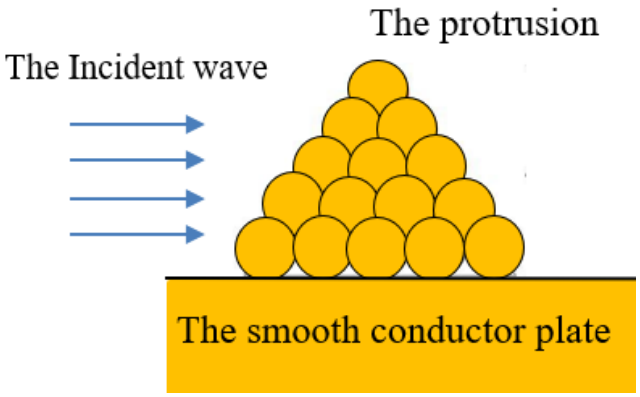

Figure 2. A protrusion consisted of stacked spheres.

As Figure 2 illustrates, for Huray model the protrusion is modeled using stacked spheres. With known number of uniform spheres (N) and under the assumption of no interaction between the spheres, the loss due to absorption is calculated using:

$$P_{abs} = N \cdot S \cdot \sigma_{abs}$$

In addition to power absorbed by the spheres, the loss due to the smooth conductor surface (P_{smooth}) needs to be taken into account. The total power loss of the rough conductor (P) is expressed therefore as:

$$P = P_{smooth} + P_{abs} = P_{smooth} + N \cdot S \cdot \sigma_{abs}$$

The power loss of a lossy conductor plate (P_{smooth}) with area equal to A_{smooth} is [10, Equ. (31)]:

$$P_{smooth} = \frac{\mu_0 \cdot \omega \cdot \delta}{4} \cdot |H_0|^2 \cdot A_{smooth}$$

where $\delta = 1/\sqrt{f\sigma\pi\mu_0}$ is the skin depth (for a non-magnetic conductor), σ is the conductivity of the conductor, and μ_0 is the permeability of free space. Typically to account for the additional power loss due to surface roughness, the resistive surface roughness correction factor (K), relating the total power loss to the loss due to the smooth conductor, is defined [4, Equ. (9)]:

$$K = \frac{P}{P_{smooth}}$$

By inserting the expressions of P and P_{smooth} shown above, the expression of K is shown below.

$$K = 1 + \frac{2 \cdot \eta \cdot N}{\mu_0 \cdot \omega \cdot \delta \cdot A_{smooth}} \cdot \sigma_{abs}$$

The absorption cross-section (σ_{abs}) of an electrically small sphere of radius a and skin depth δ can be calculated [4, Equ. (6)] as:

$$\sigma_{abs} \approx \frac{3\pi k \delta a^2}{1 + \frac{\delta}{a} + \frac{\delta^2}{2a^2}}$$

where $k = 2\pi/\lambda$, $\lambda = c \cdot (f\sqrt{\varepsilon_r})^{-1}$, c is the speed of light and ε_r is the dielectric permittivity. Notice that the surface roughness correction factor expressed by (7) is independent of the dielectric material property because ε_r is canceled out by the product of $\eta = \sqrt{\mu_0/\varepsilon_0\varepsilon_r}$ and σ_{abs}.

In recent years, Huray model has gained popularity. Good correlation with measurement results for frequencies up to 50GHz has been shown after the empirical curve fitting or tuning process. However, for Huray model, the loss of the pyramidal stack is calculated by the superposition of power absorbed from each sphere completely exposed to the incident wave, which may not be true especially when considering that the spheres shielded or hidden beneath other spheres are supposed to account for less loss than the spheres fully exposed to the wavefront.

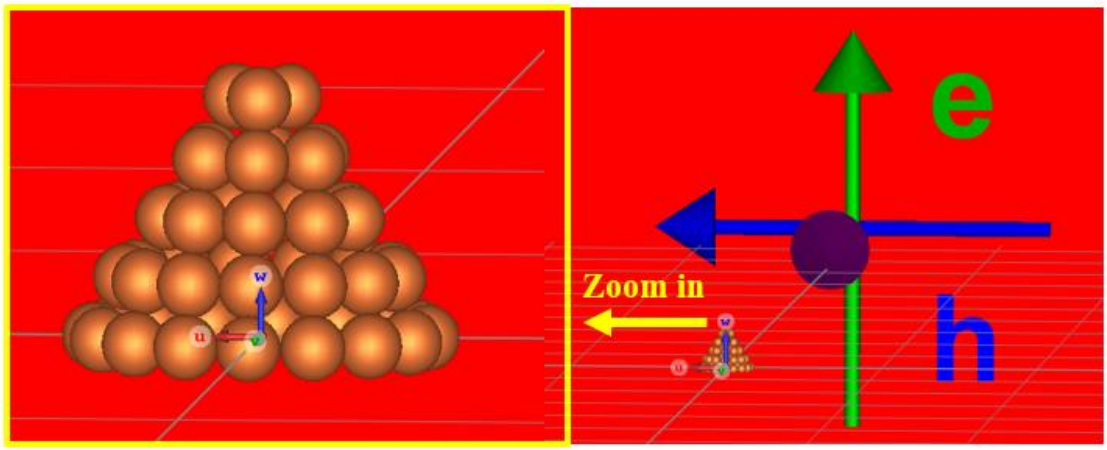

Figure 3. The absorption of the pyramidal stacked spheres is calculated using CST

To investigate the interaction among conductive structures a test is designed and illustrated in Figure 3. A protrusion exposed to the TEM wave, and consisted of pyramidal stacked copper spheres is created (the radius of the spheres r=0.3; the number

of spheres N=47). Using the CST MoM solver, the total absorption cross-section of the stacked spheres is calculated.

As the expression of P_{abs} shown above, the Huray model assumes that the interaction among stacked spheres is negligible. If such an assumption is accurate, we would be able to estimate the total absorption cross-sections of the stacked spheres by calculating the superposition of absorption cross-section from each sphere completely exposed to the incident wave. Another CST model with only one sphere exposed to the TEM is calculated, and the estimated total absorption is calculated by multiplying one sphere's absorption cross-section by the number of spheres (*N*).

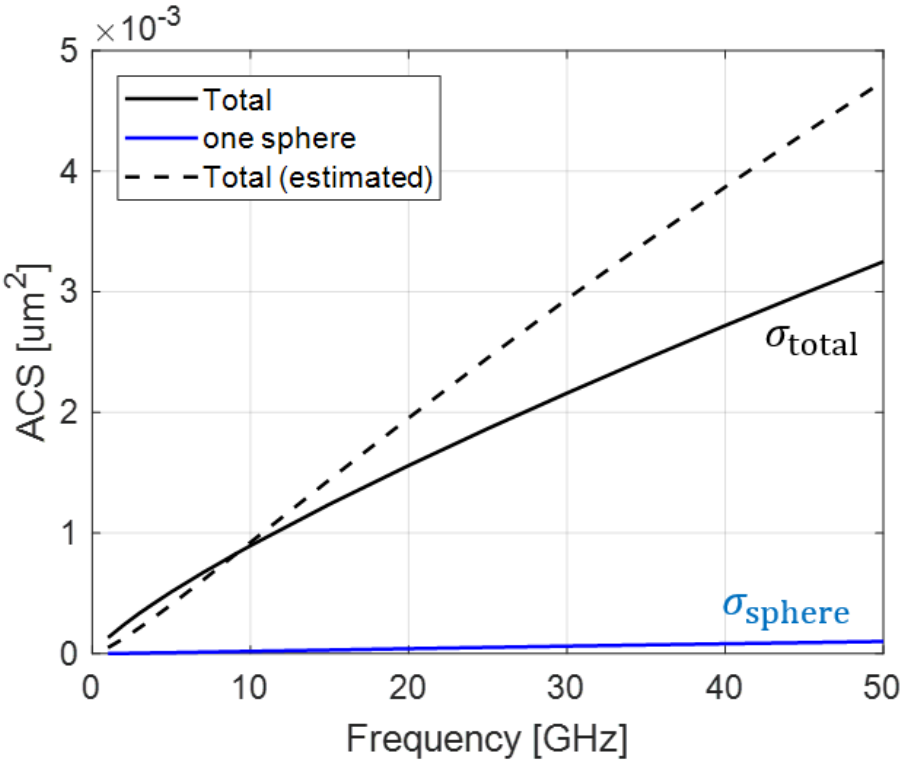

Figure 4. Absorption cross-section of the simulated protrusion consisted of stacked spheres (the black solid curve), and the estimated protrusion (the dashed curve) absorption cross-section calculated by multiplying one sphere's absorption (the blue curve) by the number of spheres (*N*=47)

We found that the estimation assuming negligible interaction among spheres severely overestimates the total absorption (Figure 4) for frequencies above 20GHz. The estimated frequency-dependence of the ACS is also more 'linear' compared to the simulation results. Thus, theoretically, it is questionable that an accurate Huray model can be built by extracting parameters only through observing SEM images. Practically it means that the set of model parameters needs to be obtained by fitting and tuning Huray model unavoidably.

The 3D Model Based on Cross-sectional Roughness Profile

A. The measured surface roughness profile

To observe the foil surface roughness, a cross-section sample of the stripline is removed from a fabricated PCB, and encapsulated in an epoxy-based compound to make the cross-section of the copper layer of interest perpendicular to the plane of view. To remove the scratches or mechanical damage caused by the cutting, the surface to be viewed is polished with sandpaper and diamond polishing compound until the metal surfaces are shiny and no obvious scratches on the surfaces can be observed using an optical microscope.

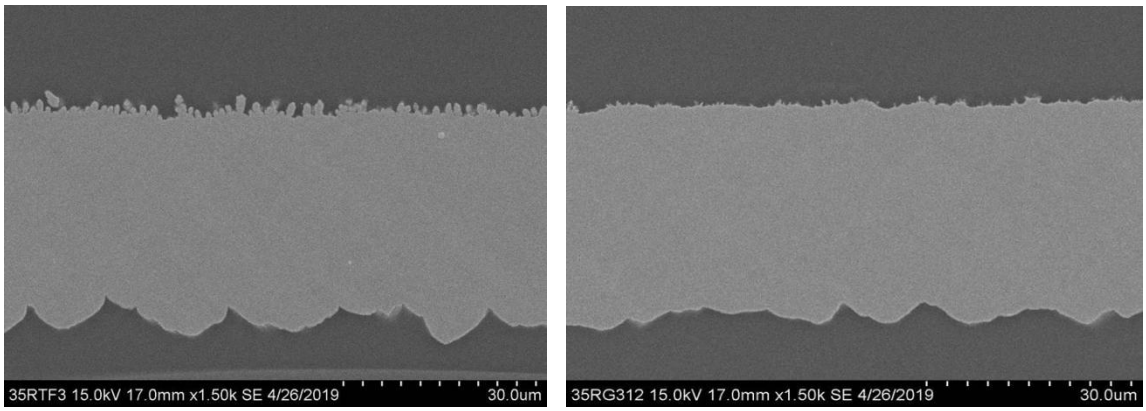

(a) (b)

Figure 5. SEM images of the cross-sectional sample of (a) conventional RTF copper foil, and (b) RG312 copper foil. The upper sides of the copper foils are under test.

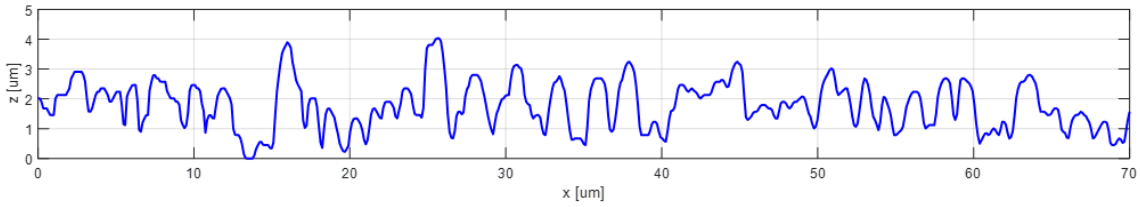

(a)

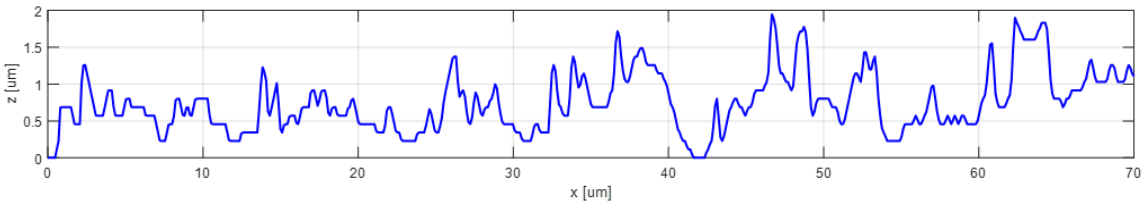

(b)

Figure 6. The cross-sectional profiles of (a) conventional RTF copper foil, and (b) RG312 copper foil. The sampling length is equal to 70 μm.

The SEM images of the conventional RTF and RG312 copper foils are illustrated in Figure 5, and the upper sides of the copper foil are used under test. An in-house image identification software is used to distinguish the transition between the copper (the lighter grey area in the middle area of Figure 5) and dielectric material (the darker grey area). The cross-section surface roughness profile data is extracted from the SEM image and illustrated in Figure 6.

By comparing Figure 6 (a) and (b), we can observe that RTF copper file is with significantly larger protrusions with averaged protrusion height equal to 1.78μm (also known as R_a, the averaged peak-to-valley height would be twice R_a value), and RG312 is with smaller averaged protrusion height 0.75 μm. On the other hand, it seems that RG312 has more 'flat' areas (for example, the area with protrusion height below 0.5 μm). and RTF copper has denser protrusions on the sampling area.

B. The Statistical Protrusion Height and The Profile Length

Before introducing the surface roughness modeling approach based on 3D simulation, let's take a look at the derivation of Huray model once again to have a better understating of the major contributors of the surface roughness correction factor, so the generated 3D model can mimic the electrical performance of the copper foil.

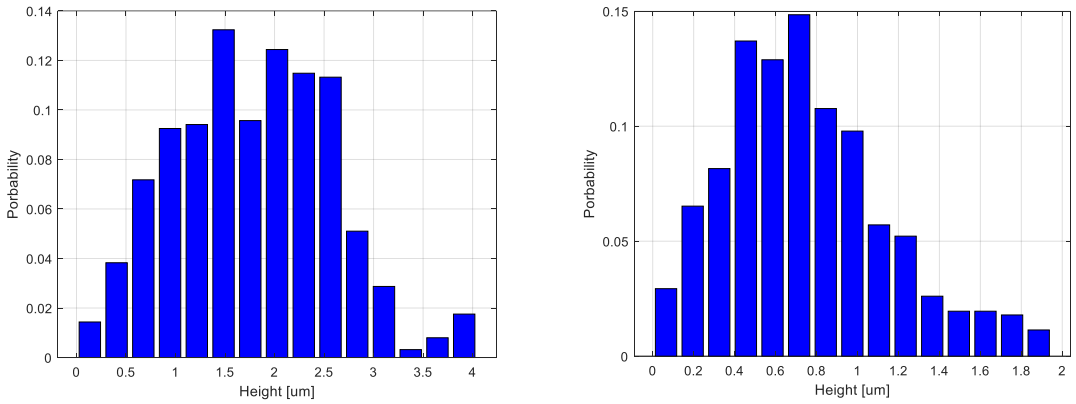

(a) (b)

Figure 7. The histogram plot of the protrusion height of (a) conventional RTF copper foil (b) RG312 copper foil. The y-axis is the relative probability, and the sum of bar heights is equal to 1.

First of all, the frequency-dependent part of the surface roughness correction factor (K) is proportional to the absorption cross-section of the conductive protrusion exposed to the TEM wave. Using Huray model as an example, a larger sphere leads to significantly larger absorption cross-section [4, Fig. 2]. Thus, the height of the protrusions is one of the most important factors for the modeling. To characterize the protrusion height information comprehensively, we analyze the cross-sectional roughness profile

statistically. The Probability Density Function (PDF) in terms of the protrusion height is calculated.

Using the cross-sectional profile information illustrated in Figure 6, the histogram plots of the protrusion height of RTF and RG312 are shown in Figure 7. It is very obvious that the conventional RTF is distributed at a higher protrusion height compared to RG312.

Secondly, the frequency-dependent part of the surface roughness correction factor (K) is also related to the number of protrusions in a certain area. Using Huray model as an example, denser spheres lead to larger correction factors. Also, the absorption cross-section (σ_{abs}) of a sphere is approximately proportional to the surface area of the sphere (a^2), so the absorption cross-section may be estimated using the equivalent surface area. Inspired by RSAR (roughness surface area ratio) shown in [11], the profile length above a certain sampling length is illustrated in Figure 8. After the statistical protrusion height information is determined by the histogram, the profile length will be used to determine the density of the protrusions.

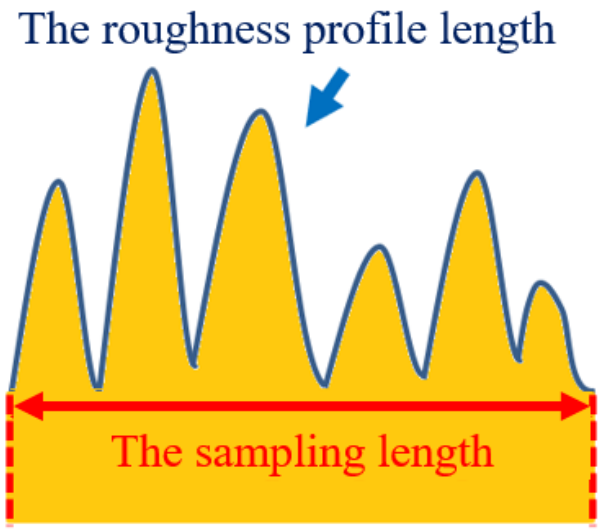

Figure 8. The illustration of the roughness profile length (the blue curve) and the sampling length (the red line with two arrows).

For the surface roughness profile plots shown in Figure 6, both plots are with sampling length equal to 70 μm. For RTF copper foil, the roughness profile length is equal to 142.3 μm, and RG312 is with profile length equal to 90.7 μm. Considering that the protrusion heigh distribution of RTF foil is also much higher than RG312 as Figure 7 illustrated, the RTF copper foil has larger and denser protrusions compared to RG312.

In subsections A and B, we define the way to measure the surface roughness information and extract the information important to the electrical performance of the copper foil. In the following subsection, we are going to provide the methodology to generate the 3D rough surface.

C. Generation of the 3D Surface

To generate the 3D rough surface, firstly a mesh grid with the x-y size equal to the sampling length is created. On this mesh grid, a certain number of points are placed uniformly on the x-y plane, and the height of the points is mapped using the protrusion height's probability information, so the points are mimicking the protrusions.

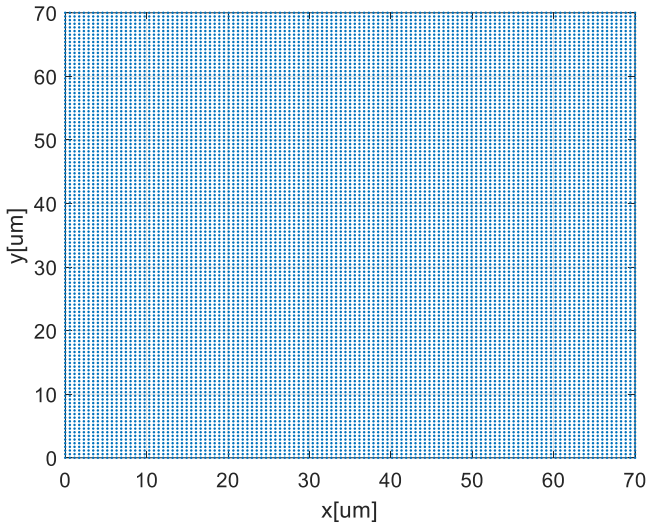

(a)

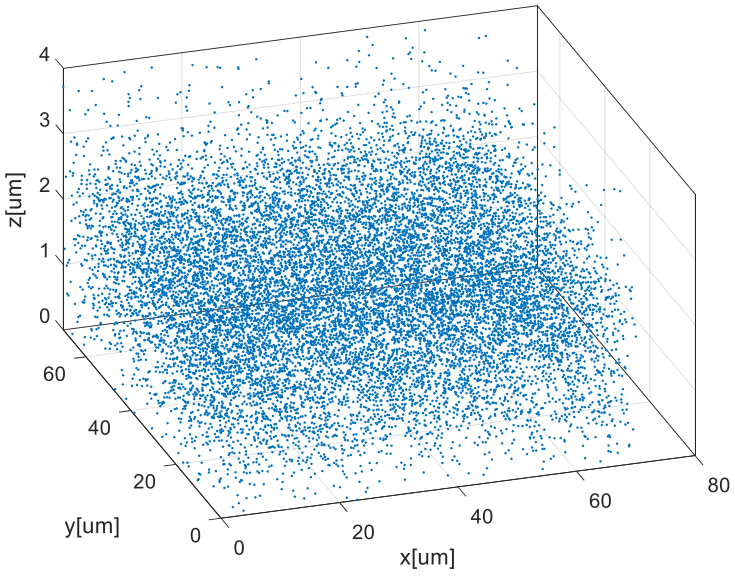

(b)

Figure 9. The (a) x-y plane view, and (b) 3D view of the points on the plane. There are 125 × 125 points with their heights assigned using the statistical information of the cross-sectional surface roughness image.

Let's use RTF copper foil as an example. The cross-sectional profile is measured and extracted as Figure 6 (a) shown, with profile length equal to 142.3 μm over the 70 μm-long sampling length. The statistical protrusion height is calculated and presented in Figure 7 (a). As Figure 9 shown, a mesh grid with size 70 μm × 70 μm is created. The number of points on the grid is equal to 125 × 125 (the method to determine the number of points will be explained later), and the points are placed uniformly on the x-y plane. Next, the height of each point is mapped using the height and probability relationship illustrated in Figure 7 (a). At last, 125 × 125 points with different height are generated on in the space as Figure 9 shown.

The next step is to create the 3D surface by interpolating 3D scatter data using the cubic method shown in Figure 9. Up till now, the height of the protrusions should match with the measured statistical protrusion height information shown in Figure 7 (a). However, the profile length may not correlate with the measured roughness profile length.

In this project, we assume that the roughness level along and perpendicular and parallel to the signal propagation direction is uniform. As Figure 10 shown, 8 cross-sectional samples are collected along with the 20/40/60/80% length of the x-axis and y-axis, and the profile length of the samples is calculated.

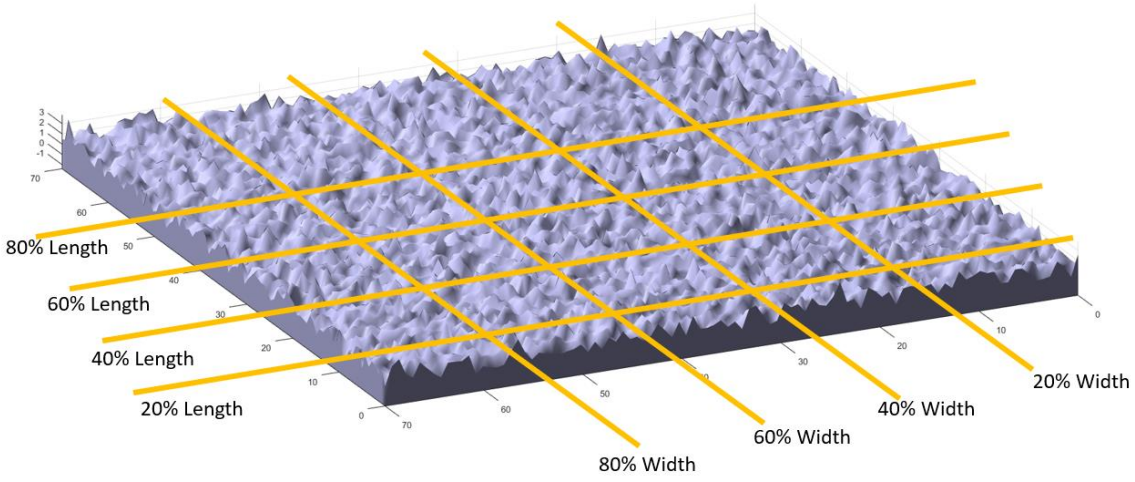

Figure 10. Check the profile length of the 3D surface generated using scattered data by sampling at 20/40/60/80% length of x and y axis.

To make the generated surface's profile length close to the measured profile length, the number of points on the mesh is adjusted. For this case with RTF foil treatment, the number of points on the grid is equal to 125 × 125, leading to a practically acceptable model and measurement profile length difference below 5% (as Table I and Figure 11 shown). Increasing the number of points leads to a denser protrusion on the sampling area, and the modeled profile length will increase significantly (for example, with 150 ×

150 points mapped using the same RTF protrusion height distribution, the averaged profile length is around 165).

Samples (x location) [μm]	Profile length [μm]	Model & Measurement Difference	Samples (y location) [μm]	Profile length [μm]	Model & Measurement Difference
13.95	139.46	2.0%	13.95	150.31	5.6%
27.96	151.49	6.5%	27.96	145.52	2.3%
41.93	136.03	4.4%	41.93	149.35	5.0%
56.02	142.82	0.37%	56.02	143.55	0.9%
Averaged x	147.18	3.4%	Averaged y	142.45	0.1%

Table 1. The generated 3D model's profile length sampled at different location at x and y axis. The difference compared to the measurement in percentage is calculated. For RTF the measured profile length is equal to 142.3 μm.

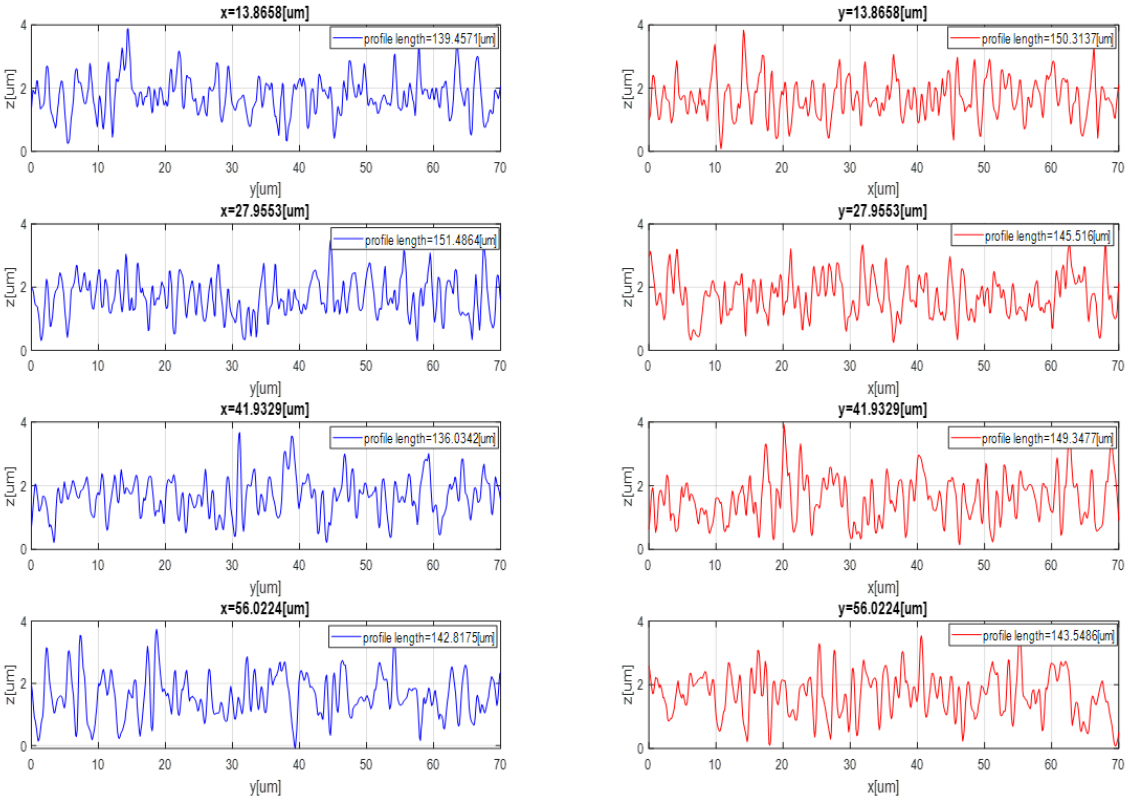

Figure 11. The cross-sectional profiles of the generated 3D model for conventional RTF copper foil.

For the current implementation, the gradient descendant algorithm is used to determine the number of points on the on the mesh grid to make difference to the averaged profile length within the range of $\pm 5\%$. Using the proposed approach, the 3D rough surfaces generated using the cross-sectional profile data of RTF and RG312 shown in Figure 6 are illustrated in the plots shown below.

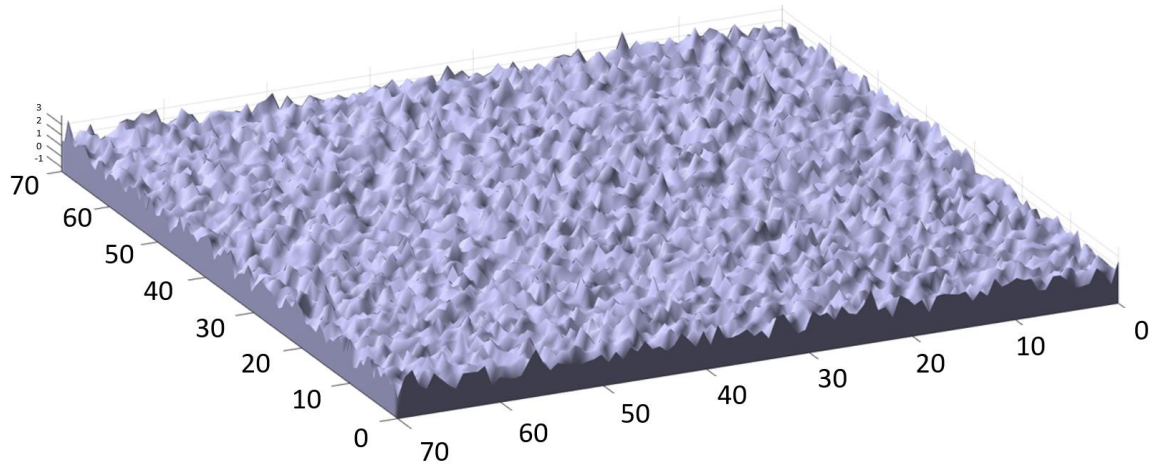

(a)

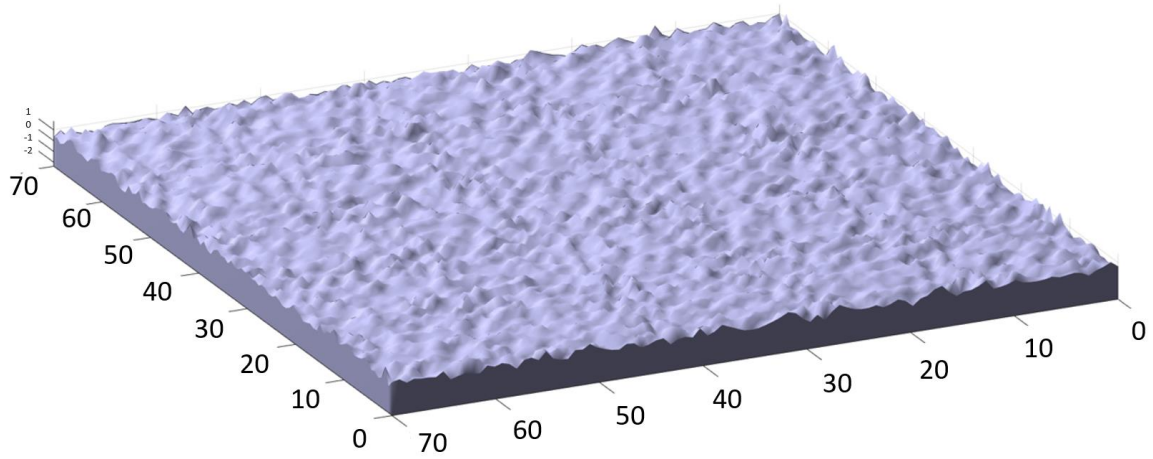

(b)

Figure 12. Generated 3D rough surface for (a) Conventional RTF, and (b) RG2312.

The generated 3D roughness surface is exported using an STL file and imported into Ansys HFSS using the modeler import functionality. As Figure 13 shown, the stripline model with rough surfaces is created. To solely characterize the conductive loss, the dielectric material is assigned as air with loss tangent equal to zero. Also, to setup the wave-ports with low reflection, the conductors close to the ports are assigned with smooth surfaces. The smooth parts close to the wave-ports are deembeded after the 3D model is solved, so only the conductors with rough surfaces are taken into account for the final solution.

At last, the insertion loss taking the rough surfaces is calculated by HFSS, and the surface roughness correction factor is obtained by calculating the ratio between the attenuation factors of the rough model and the smooth model. As a short summary, the illustration of the whole process is demonstrated in the diagram shown in Figure 14.

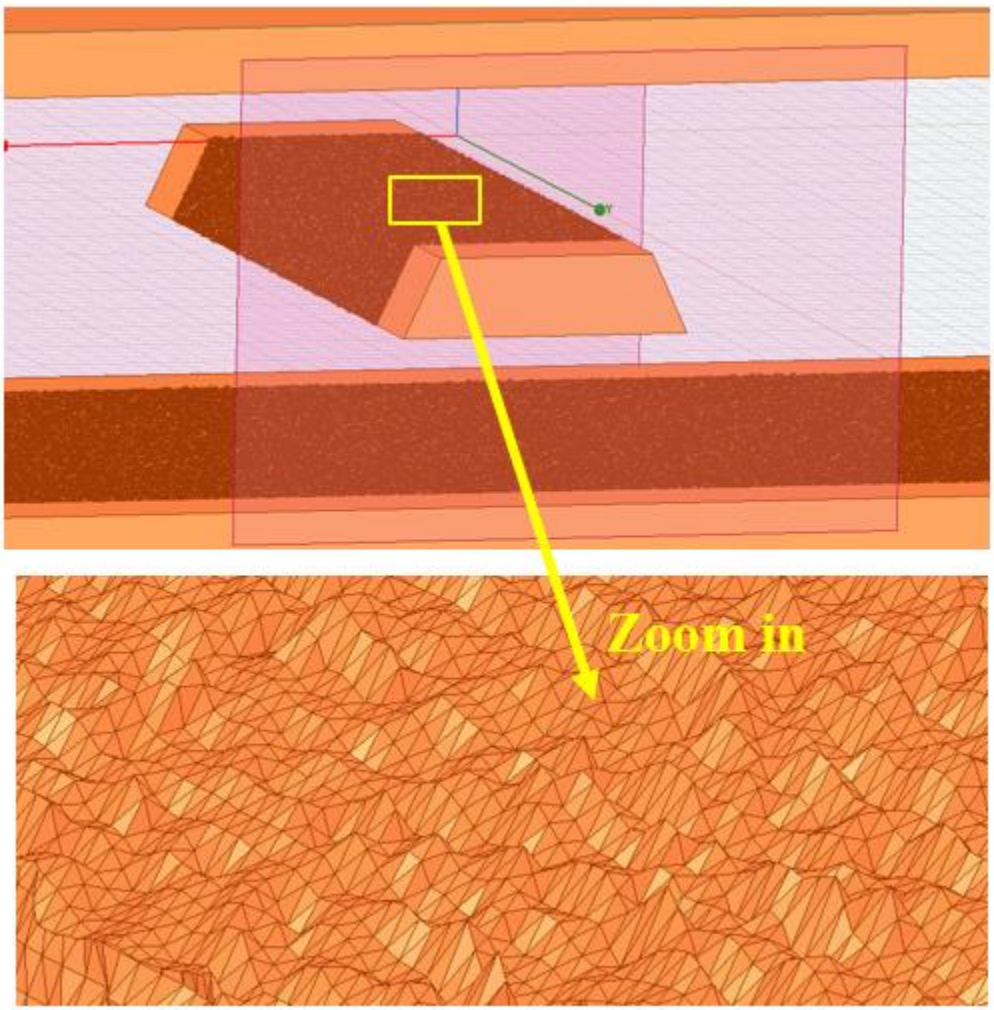

Figure 13. The HFSS 3D stripline model with conventional RTF rough surfaces is shown in the upper figure. The smooth parts close to the wave ports are de-embeded. The rough foil surface is illustrated by the lower figure.

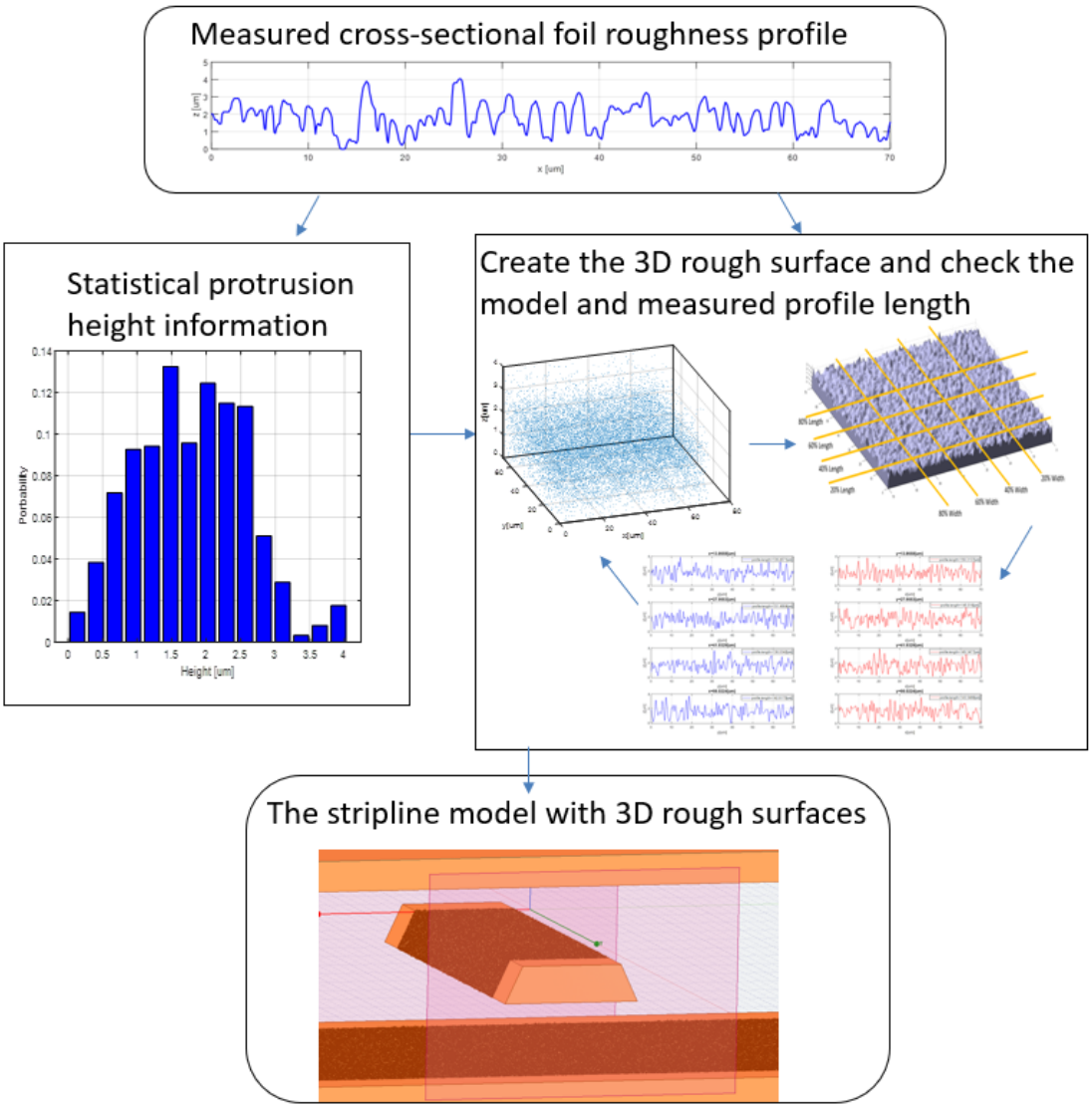

Figure 14. The diagram of the proposed surface roughness modeling approach based on 3D simulation.

Validations

To illustrate the feasibility and accuracy of the proposed method, testing boards with the same dielectric material (EM528) and four different copper foil treatments (RT330/RG311/RG312/VL41A) are fabricated (see Figure 15). For the presented implementation, we used 2X-Thru de-embedding technique [12-14] to remove the unwanted error boxes including the probe and the transition area. The cross-sectional SEM images are presented in Figure 5 and 16.

Using the proposed surface roughness modeling approach, 3D models are created using the SEM cross-sectional roughness profile image. Different surface roughness levels on the planes of the fabricated stripline [15] are taken into account by inserting different generated surface roughness surfaces. The modeled surface roughness correction factors for four copper foil types are illustrated in Figure 17.

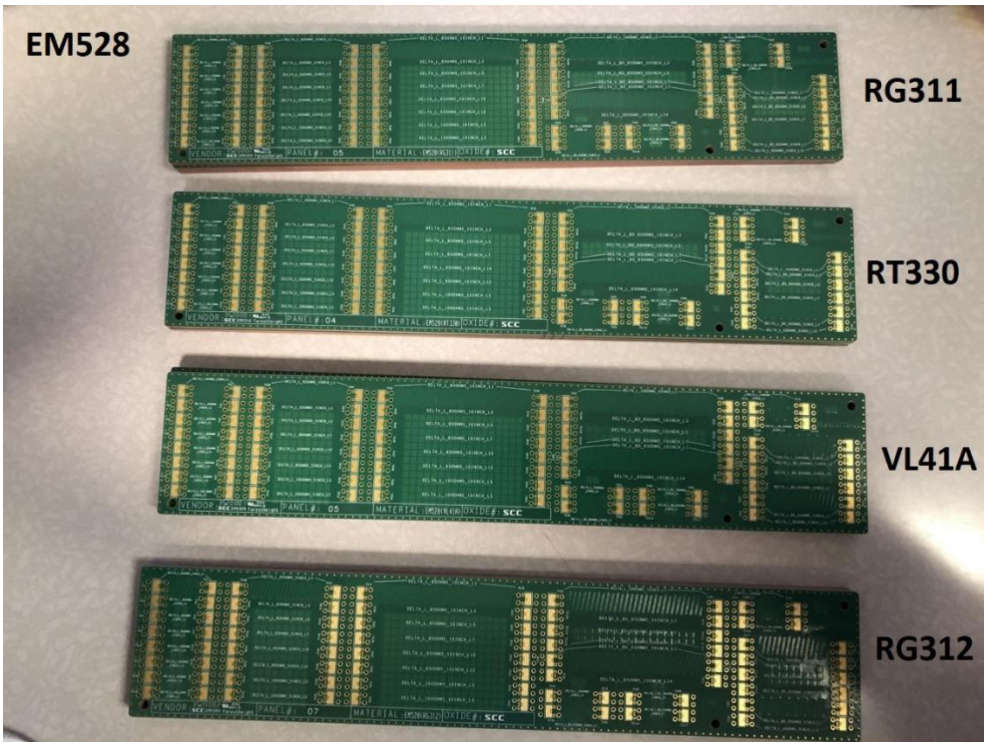

Figure 15. The testing boards with different copper coil treatment (dielectric material: EM528; Copper foil types: RT330/RG311/RG312/VL41A).

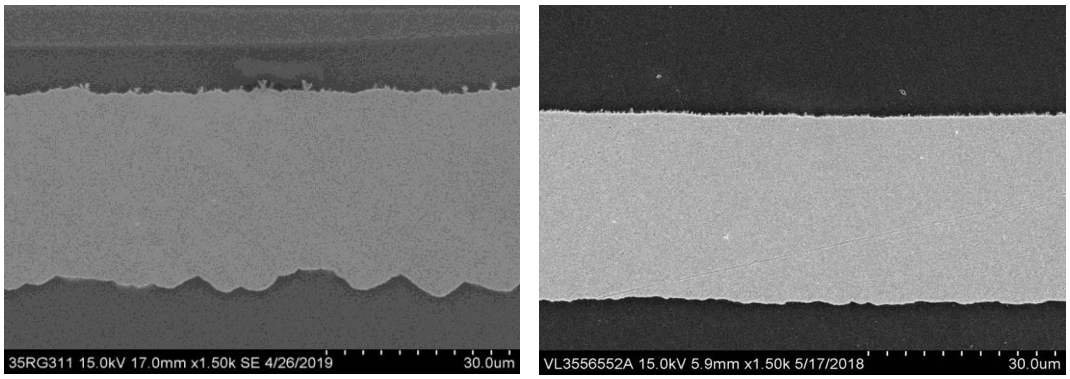

(a) (b)

Figure 16. SEM images of the cross-sectional sample of (a) RG311, and (b)VL41A copper foil. The upper sides of the copper foils are under test.

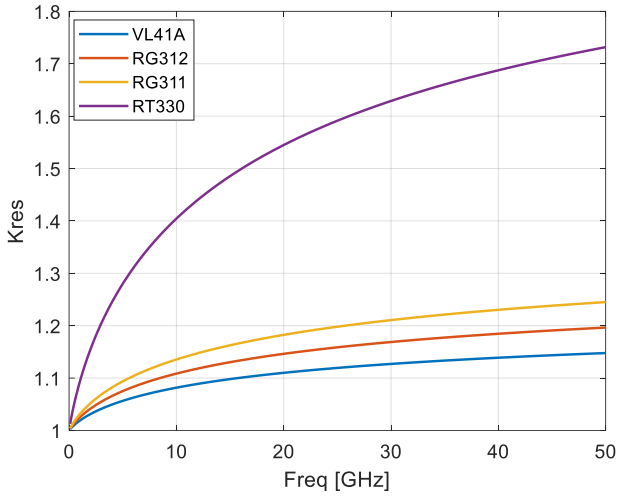

.

Figure 17. The modeled surface roughness correction factors obtained using the proposed approach for RT330, RG311, RG312 and VL41A.

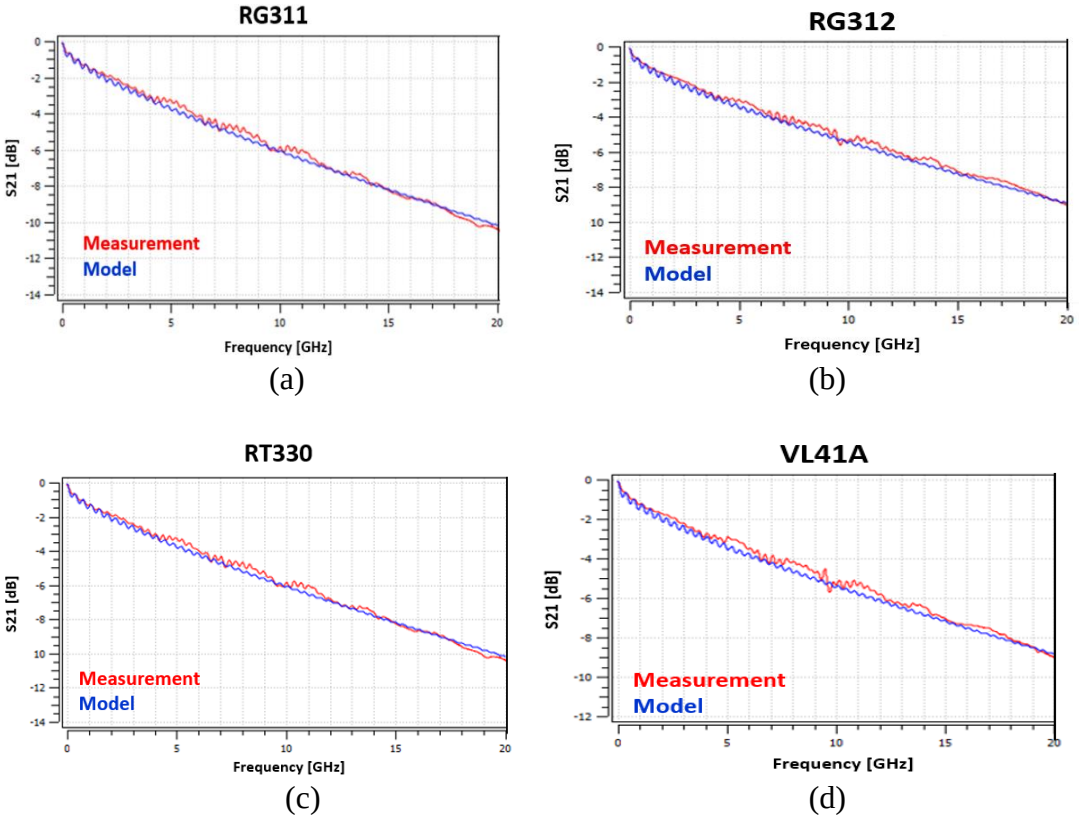

Figure 18. The comparison between the modeled and measured insertion loss for four different PCBs with different copper foil types.

The dielectric material information is extracted from the fabricated PCB using the dielectric material characterization tool [16-18]. Since all the boards are fabricated using EM528, for all four boards the extracted dielectric permeability (DK) and dielectric dissipation loss tangent (DF) is quite close (3.90-3.91 for DK; 0.0051-0.0052 for DF).

Using the extracted DK, DF, and modeled surface roughness correction factor, the modeled transmission line is created. The comparison between the modeling and measurement results is shown in Figure 18, and a pretty good correlation can be observed.

Conclusion

To achieve the improved accuracy of the copper foil characterization, the cross-sectional foil roughness SEM images of fabricated striplines are used as the only input of the proposed approach. A methodology is brought up to create a 3D rough foil surface using the measured cross-sectional roughness data. The additional conductive loss due to surface roughness is characterized by a full-wave simulation. Compared to the traditional Huray model neglecting of the interaction among spheres, the proposed approach can provide results with accurate frequency-dependence. Also, the parameter tuning process for Huray model is no longer needed.

Bibliography

[1] B. Chen, S. Pan, J. Wang, S. Yong, M. Ouyang and J. Fan, "Differential Crosstalk Mitigation in the Pin Field Area of SerDes Channel With Trace Routing Guidance," in *IEEE Transactions on Electromagnetic Compatibility*, vol. 61, no. 4, pp. 1385-1394, Aug. 2019

[2] S. Yong, V. Khilkevich, X. Cai, C. Sui, B. Sen and J. Fan, "Comprehensive and Practical Way to Look at Far-End Crosstalk for Transmission Lines With Lossy Conductor and Dielectric," in *IEEE Transactions on Electromagnetic Compatibility*, vol. 62, no. 2, pp. 510-520, April 2020

[3] S. Penugonda, S. Yong, A. Gao, K. Cai, B. Sen and J. Fan, "Generic Modeling of Differential Striplines Using Machine Learning Based Regression Analysis," *2020 IEEE International Symposium on Electromagnetic Compatibility & Signal/Power Integrity (EMCSI)*, 2020, pp. 226-230

[4] P. G. Huray, O. Oluwafemi, J. Loyer, E. Bogatin, X. Ye, "Impact of Copper Surface Texture on Loss: A Model that Works", *DesignCon 2010*.

[5] Y. Shlepnev, "Unified approach to interconnect conductor surface roughness modelling", *in 2017 IEEE 26st Conference on Electrical Performance of Electronic Packaging and Systems (EPEPS2017)*, San Jose, CA

[6] Y. Chu, "Method for modeling conductor surface roughness", US Patent#8527246.

[7] S. Yong et al., "A Cross-sectional Profile Based Model for Stripline Conductor Surface Roughness," *2020 IEEE International Symposium on Electromagnetic Compatibility & Signal/Power Integrity (EMCSI)*, 2020, pp. 334-339.

[8] S. Hall, S. G. Pytel, P. G. Huray, D. Hua, A. Moonshiram, G. A. Brist, and E. Sijercic "Multigigahertz Causal Transmission Line Modeling Methodology Using a 3-D Hemispherical Surface Roughness Approach", *IEEE Trans. Microw. Theory Tech.*, vol. 55, no. 12, Dec. 2007, pp. 2614 – 2624.

[9] Jackson, J. D., "Classical Electrodynamics", 3rd edition. Wiley, New York, 1999.

[10] S. Hall, S. G. Pytel, P. G. Huray, D. Hua, A. Moonshiram, G. A. Brist, and E. Sijercic "Multigigahertz Causal Transmission Line Modeling Methodology Using a 3-D Hemispherical Surface Roughness Approach*", IEEE Trans. Microw. Theory Tech.*, vol. 55, no. 12, Dec. 2007, pp. 2614 – 2624.

[11] John A. Marshall, "Measuring Copper Surface Roughness for High Speed Applications,". Published in the *IPC proceedings*.

[12] Q. Huang, J. Li, J. Zhou, W. Wu, Y. Qi, and J. Fan, “De-embedding method to accurately measure high-frequency impedance of an O-shape spring contact,” in *Proc. Int. Symp. IEEE Electromagn. Compat*., 2014, pp. 600– 603.

[13] Y. Liu et al., "S-Parameter De-Embedding Error Estimation Based on the Statistical Circuit Models of Fixtures," in *IEEE Transactions on Electromagnetic Compatibility*, vol. 62, no. 4, pp. 1459-1467, Aug. 2020.

[14] S. Yong et al., "A Practical De-embedding Error Analysis Method Based on Statistical Circuit Models of Fixtures," *2019 IEEE International Symposium on Electromagnetic Compatibility, Signal & Power Integrity (EMC+SIPI)*, 2019, pp. 45-50.

[15] S. Yong et al., "Resistance Modeling for Striplines with Different Surface Roughness on the Planes," *2020 IEEE International Symposium on Electromagnetic Compatibility & Signal/Power Integrity (EMCSI)*, 2020, pp. 340-345.

[16] Advanced Interconnect Test Tool (AITT) (https://clearsig.com/clearsig/)

[17] S. Yong et al., "Dielectric Material and Foil Surface Roughness Properties Extraction Based on Single-ended Measurements and Phase Constant (β) Fitting," *2020 IEEE International Symposium on Electromagnetic Compatibility & Signal/Power Integrity (EMCSI)*, 2020, pp. 346-351.

[18] S. Yong et al., "Dielectric Loss Tangent Extraction Using Modal Measurements and 2-D Cross-Sectional Analysis for Multilayer PCBs," in *IEEE Transactions on Electromagnetic Compatibility*, vol. 62, no. 4, pp. 1278-1292, Aug. 2020.